

# ADVANCES in WOUND CARE

Advances in Wound Care : <http://mc.manuscriptcentral.com/whsyb>

## Assessment of transdermal delivery of topical compounds in skin scarring using a novel combined approach of Raman spectroscopy and HPLC

Journal:	<i>Advances in Wound Care</i>
Manuscript ID	WOUND-2020-1154.R1
Manuscript Type:	Technology Advances
Date Submitted by the Author:	11-Apr-2020
Complete List of Authors:	Basson, Rubinder; university of manchester, Plastics and Reconstructive Surgery Lima, Cassio; University of Liverpool Institute of Integrative Biology Muhamadali, Howbeer; University of Liverpool Institute of Integrative Biology Li, Weiping; The University of Manchester Hollywood, Katherine; University of Manchester Institute of Science and Technology Department of Biomolecular Science Li, Ludanni; The University of Manchester Baguneid, Mo; Al Ain Hospital Al Kredly, Rawya; Julphar Goodacre, Royston; University of Liverpool Institute of Integrative Biology Bayat, Ardeshir; University of Manchester, Plastic & Reconstructive Surgery Research, Manchester Institute of Biotechnology; Wythenshawe Hospital, Department of Plastic and Reconstructive Surgery, University Hospital South Manchester NHS Foundation Trust
Keyword:	Acute Wound, Biomarkers, Clinical Trials, Extracellular Matrix
Manuscript Keywords (Search Terms):	transdermal delivery, skin scarring, topicals, HPLC, Raman spectroscopy, Wound healing

SCHOLARONE™  
Manuscripts

1  
2  
3 Article type: Technology advances  
4

5 **Assessment of transdermal delivery of topical compounds in skin scarring**  
6 **using a novel combined approach of Raman spectroscopy and HPLC**  
7  
8  
9

10  
11  
12 Rubinder Basson<sup>1</sup>, Cassio Aparecido Lima<sup>2</sup>, Howbeer Muhamadali<sup>2</sup>, Weiping Li<sup>1</sup>,  
13 Katherine Hollywood<sup>3</sup>, Ludanni Li<sup>1</sup>, Mohamed Baguneid<sup>4</sup>, Rawya Al Kredy<sup>5</sup>, Royston  
14 Goodacre<sup>2</sup>, Ardeshir Bayat<sup>1\*</sup>  
15  
16  
17  
18  
19

20  
21 1. Plastic and Reconstructive Surgery Research, Centre for Dermatology Research,  
22 NIHR, Manchester Biomedical Research Centre, University of Manchester, UK.  
23

24 2. Department of Biochemistry, Institute of Integrative Biology, University of Liverpool,  
25 UK.  
26  
27

28 3. Synbiochem, Manchester Institute of Biotechnology, Manchester, UK  
29

30 4. Al Ain Hospital, SEHA, Abu Dhabi Emirate, UAE  
31

32 5. Julphar Gulf Pharmaceutical Industries, UAE  
33  
34  
35  
36  
37  
38  
39

40 \*Corresponding author and reprint requests:  
41

42 Dr. Ardeshir Bayat  
43

44 Plastic and Reconstructive Surgery Research, Centre for Dermatology Research,  
45 NIHR Biomedical Research Centre, University of Manchester, England, United  
46 Kingdom. Tel: +44 161 2750 209 Email: ardeshir.bayat@manchester.ac.uk  
47  
48  
49  
50  
51  
52

53 Running head: Transdermal delivery of topicals in skin scarring  
54

55 Key words: Transdermal delivery, skin scarring, topicals, HPLC, Raman spectroscopy,  
56 wound healing.  
57  
58  
59  
60

## Abstract

**Objective:** The goal of any topical formulation is efficient transdermal delivery of its active components. However, delivery of compounds can be problematic with penetration through tough layers of fibrotic dermal scar tissue.

**Approach:** We propose a new approach combining high performance liquid chromatography (HPLC) and Raman spectroscopy (RS) using a topical of unknown composition against a well-known anti-scar topical (as control).

**Results:** Positive detection of compounds within the treatment topical using both techniques was validated with mass spectrometry. RS detected conformational structural changes; the 1655/1446  $\text{cm}^{-1}$  ratio estimating collagen content significantly decreased ( $p < 0.05$ ) over weeks (W) 4, 12, and 16 compared to Day (D) 0. The amide I band, known to represent collagen and protein in skin, shifted from 1667  $\text{cm}^{-1}$  to 1656  $\text{cm}^{-1}$  which may represent a change from  $\beta$ -sheets in elastin to  $\alpha$ -helices in collagen. Confirmatory elastin immunohistochemistry decreased compared to D0, conversely the collagen I/III ratio increased in the same samples by W12 ( $p < 0.05$ , and  $p < 0.0001$  respectively), in keeping with normal scar formation. OCT attenuation coefficient representing collagen deposition was significantly decreased at W4 compared to D0 and increased at W16 ( $p < 0.05$ ).

**Innovation:** This study provides a platform for further research on the simultaneous evaluation of the effects of compounds in cutaneous scarring by RS and HPLC, and identifies a role for RS in the therapeutic evaluation and theranostic management of skin scarring.

**Conclusions:** RS can provide non-invasive information on the effects of topicals on scar pathogenesis and structural composition, validated by other analytical techniques.

## Introduction

The goal of any topical formulation should be efficient transdermal delivery of its actives in order to address the signs and symptoms of abnormal skin scarring.<sup>1</sup> There are 3 basic layers that make up skin: the outermost epidermis, the dermis (divided into an upper papillary layer and a thicker reticular layer) which extends into the inner hypodermis (fatty layer).<sup>2</sup> The dermis contains all the connective tissue components and provides the tensile strength and elasticity of the skin, which are altered through the remodelling process of scarring.<sup>3</sup> Separating the dermis from the epidermis is a basement membrane.<sup>3</sup> Upon wounding, there is disruption of the layers, resulting in a loss of structure, and a replacement with scar tissue.<sup>3</sup> As there is no reconstitution back to its original state, the resultant scar formed may be linear, depressed (atrophic), contracted or raised (hypertrophic or keloid) manifesting in a range of symptoms including erythema, pruritus, and pigmentation; and as such, responsible for the significant retail market for anti-scar treatments.<sup>4</sup>

The commonly utilised treatments include the use of inert silicone gels, oils and sheets shown to provide hydration by occlusion.<sup>5</sup> Other widely used topicals claim to provide moisturization for symptomatic relief of dryness, for example aloe vera<sup>6</sup> and vitamin E,<sup>7</sup> or scar reduction with improvement in redness and elasticity, using topicals containing compounds with anti-inflammatory properties such as epigallocatechin gallate (EGCG),<sup>8</sup> and formulas such as MEBO (moist exposure burn ointment) Scar ointment originally developed for used during burn treatment.<sup>9</sup>

Delivery of active compounds, however, can be problematic with penetration of the stratum corneum of normal skin let alone through abnormal dermal scars containing

1  
2  
3 excessive fibrous tissue. Current widely used methods for assessment of transdermal  
4 delivery of active compounds include: the use of high-performance liquid  
5 chromatography (HPLC) and mass spectrometry (MS). MS is commonly used to  
6 validate HPLC findings as it provides confirmation of the active ingredient(s),<sup>10</sup> and  
7 LC-MS (liquid chromatography- mass spectrometry) has even been used to  
8 validate Fourier transform infra-red (FTIR) spectroscopy analysis of the human skin  
9 barrier.<sup>11</sup>

10  
11  
12  
13  
14  
15  
16  
17  
18  
19  
20  
21 Another useful method for detection of, and assessment of, transdermal delivery of  
22 active compounds is Raman spectroscopy (RS) which is a non-destructive, vibrational  
23 spectroscopic technique that is used to probe the molecular changes within biological  
24 tissue.<sup>12</sup> RS is a vibrational spectroscopic method that provides a biomolecular  
25 fingerprint for macromolecules, which contains both chemical information and physical  
26 information. As shown by Mendelsohn's group when conformational changes occur  
27 in tissue development, disease, repair, or regeneration, they manifest in the spectra.<sup>13</sup>  
28 RS is not only used for assessment of transdermal delivery but in both basic research  
29 and in the clinical setting, where analysis of normal skin composition has been  
30 demonstrated, as shown by a recent study<sup>14</sup> that used RS to obtain quantitative, non-  
31 invasive spectral data on skin thickness. Successful discrimination between layers of  
32 the epidermis which is normally affected after formalin-fixation (and is also invasive),  
33 was evidenced due to the higher spatial resolution of RS (1  $\mu\text{m}$  is typical) than other  
34 non-invasive techniques such as high frequency ultrasound (HFUS) and optical  
35 coherence tomography (OCT).<sup>14</sup>

36  
37  
38  
39  
40  
41  
42  
43  
44  
45  
46  
47  
48  
49  
50  
51  
52  
53  
54  
55  
56  
57  
58  
59  
60

### Clinical problem addressed

Topical treatments are the mainstay of management options for the prevention and symptomatic relief of scars; a high number of which are over-the-counter remedies. Despite the abundance of topicals on the market, limited scientific evidence exists for their effect. Penetration through tough fibrotic scar tissue remains problematic in the assessment of anti-scar topical formulations, and the perceived lack of a robust methodology to assess transdermal delivery of their actives presents further difficulties in providing objective and quantitative analysis. We present a combined approach to the assessment of transdermal delivery of topicals, whilst synergistically providing information on the conformational changes taking place within the dermal scar tissue which is corroborated by conventional histological techniques.

To demonstrate the clinical application of RS in the assessment of skin scarring we assess transdermal delivery of a topical (MEBO Scar ointment),<sup>9</sup> which has an unknown mechanism of action and no proven known 'actives'. First, using an *ex vivo* human skin organ culture model, utilising the traditional method of HPLC.<sup>15</sup> This technique confirmed the presence of two compounds, tyramine, and linoleic acid, and their delivery could be evidenced within the different dermal layers; the confirmatory presence of these compounds was validated by MS. Effective transdermal delivery was then observed using RS. To validate these findings, the same techniques were applied on *in vivo* skin samples obtained from a clinical trial with the same topical and compared to a positive control, (kelo-cote®).<sup>16</sup> Kelo-cote® was selected, as silicone-based topicals are most commonly used in clinical practice and their effect shown to be positive in skin scarring as evidenced by a Cochrane Review.<sup>17</sup>

1  
2  
3 We therefore, hypothesised that a combi-approach of techniques, allows for  
4 successful validation of transdermal delivery of a topical even though the compounds  
5 within the treatment topical remain unknown, with additional information on  
6 conformational changes within the scar tissue. Figure 1 demonstrates the  
7 experimental workflow for this study; Part A represents the *ex vivo*, and B, the *in vivo*  
8 components of the study.  
9  
10  
11  
12  
13  
14  
15  
16  
17  
18  
19  
20  
21  
22  
23  
24  
25  
26  
27  
28  
29  
30  
31  
32  
33  
34  
35  
36  
37  
38  
39  
40  
41  
42  
43  
44  
45  
46  
47  
48  
49  
50  
51  
52  
53  
54  
55  
56  
57  
58  
59  
60

## Materials and Methods

### *Ex vivo* human skin organ culture model

We utilised the culture method previously validated and evidenced by our group.<sup>15</sup>

Discarded human skin samples were obtained from patients undergoing routine aesthetic surgery such as abdominoplasty, who were consented prior to their procedure with ethical approval (16/NW/0736) from the University of Manchester. All tissue was tracked and stored in a human tissue biobank following Human Tissue Act (HTA) guidelines. Skin was obtained from six patients; three samples were non-scarred, i.e. 'normal' skin, and three were 'scarred' skin samples.

After trimming the excess hypodermal fat, circular organ culture explants were prepared with a 6 mm biopsy punch (Kai Medical, Japan). The biopsies were transferred to a 24-well plate containing transwell inserts (Corning®, USA), allowing them to be suspended in the culture media whilst keeping the epidermis exposed to the air-liquid interphase, for the addition of the treatment. Each biopsy was cultured in 500 µL of Williams E culture media (Gibco™, USA) supplemented with 1% penicillin/streptomycin, 1% L-glutamine, 1% none-essential amino acid solution, 1% ITS+3, and 10 ng/mL hydrocortisone. The culture medium was changed daily, and the biopsies were maintained at 37°C in a humidified incubator with a 5% CO<sub>2</sub> atmosphere.

### Topical formulations

MEBO Scar ointment (Julphar Pharma, UAE), comprising sesame, cactus, and beeswax, was originally formulated in China from its derivative MEBO™ (moist exposed burn ointment), (Julphar Pharma, UAE).<sup>9</sup> MEBO Scar claims to possess at



1  
2  
3 least two compounds, tyramine, and linoleic acid, (unknown actives) which are thought  
4 to improve skin scarring through an enhanced remodelling process and improved  
5 microcirculation.<sup>9</sup> In this study we aim to demonstrate the presence of these  
6 compounds through dermal scar tissue using the combined aforementioned  
7 techniques. Kelo-cote<sup>®</sup> (Sinclair Pharma, UK), comprising 100% silicone-base was  
8 used a positive control.  
9  
10  
11  
12  
13  
14  
15  
16  
17  
18

### 19 **Assessment of transdermal delivery using *ex vivo* samples**

21 'Normal' skin *ex vivo* organ culture samples were used to assess transdermal delivery  
22 of tyramine and linoleic acid. The biopsies were divided into 3 groups ( $n=9$ ). The first  
23 group had 5  $\mu\text{L}$  of the treatment topical applied to the epidermis, the second group  
24 had 5  $\mu\text{L}$  of the positive control applied, whilst the control group had neither topical  
25 applied. On days 0, 3, 7, and 10; the biopsies were washed with PBS (Phosphate-  
26 buffered Saline) and then snap frozen and stored at  $-80^{\circ}\text{C}$  ready for further analysis.  
27  
28  
29  
30  
31  
32  
33  
34  
35  
36  
37

### 38 **HPLC**

39  
40 This was also based on the methodology previously demonstrated by our group.<sup>15</sup>  
41 Three samples for each condition ( $n=9$ ) were used for the *ex vivo* experiments, and  
42  $n=15$  for the *in vivo* (3 for each time point, day 0, treatment topical at weeks 8, 12 and  
43 16, and positive control topical at week 12). An optimised Agilent 1100 system,  
44 (Agilent Tech, USA) was utilised, and data analysis performed using ChemStation  
45 (Agilent Tech, USA) software. Pure linoleic acid and tyramine (Sigma-Aldrich, UK)  
46 were tested at different concentrations (100mM, 10mM, 100 $\mu\text{M}$ , 10 $\mu\text{M}$ ), with a column  
47 (Sphereclone), (Phenomenex Inc, USA) ideal size of 4.6 x 250mm, to generate  
48 standard curves for quantification. The solvent condition was acetonitrile at different  
49  
50  
51  
52  
53  
54  
55  
56  
57  
58  
59  
60

1  
2  
3 concentrations (20%, 40%, 70%, 80%, and 90%) with 1% TFA (trifluoroacetic acid).  
4  
5 The flow rate was 1ml/min at 10, 50, and 100  $\mu$ L volumes. Detection of linoleic acid  
6  
7 tyramine was at 225 nm wavelength, at 6 min and 2 min respectively.  
8  
9

## 10 11 12 **Mass Spectrometry**

13  
14 Skin tissue was weighed to ensure it was less than 25 mg. A total of 9 samples from  
15  
16 different conditions were used, treatment, control, and day 0 (no treatment). Aliquots  
17  
18 (1 mL of hexane and isopropanolol, at a ratio of 3:2 was added to each sample), and  
19  
20 was homogenised in a tissue lyser (Quiagen UK), then centrifuged at 15890 *g* for 15  
21  
22 min. The supernatant was collected for MS. All analysis was conducted on a  
23  
24 QExactive Plus coupled with an Ultimate 3000 UHPLC (Thermo, UK). The UHPLC  
25  
26 was equipped with an Accucore Vanquish reverse phase column (C18 -2.1 mm x 100  
27  
28 mm; 1.5 mm particle size). The solvents employed were (A) water + 0.1% formic acid  
29  
30 and (B) methanol + 0.1 % formic acid. The flow gradient was programmed to  
31  
32 equilibrate at 98% A for 2 min followed by a linear gradient to 95% B over 10 min and  
33  
34 held at 95% B for 2 min before returning to 95% A for 2 min. The flow rate was  
35  
36 300 mL/min. The column was maintained at 40 °C and the samples chilled in the auto-  
37  
38 sampler at 45 °C. A sample volume of 5  $\mu$ L was injected into the column. Data  
39  
40 acquisition was conducted in full MS mode in the scan range of 90-1350 *m/z* with a  
41  
42 resolution of 70,000, an AGC target of  $3e^6$  and a maximum integration time of 100 ms.  
43  
44 The samples were analysed in positive (tyramine) and negative mode (linoleic acid) in  
45  
46 separate acquisitions.  
47  
48  
49  
50  
51  
52  
53  
54  
55  
56  
57  
58  
59  
60

### **Clinical trial for *in vivo* human skin samples**

Forty-five subjects were recruited and followed up over a period of 8 months, in order to evaluate the role of Mebo Scar (Julphar Pharma, UAE) in skin scarring.<sup>17</sup> Samples from twenty of these subjects were used for assessment of transdermal delivery using RS. All subjects signed a written consent form, (UREC ref 16098), in addition to verbally consenting at each visit in keeping with the declaration of Helsinki principles. Sample size and study power was determined by an independent statistician from the University of Manchester, considering all background variables, and samples equally distributed with no bias. Recruitment was via the University volunteer intranet pages. All subjects were fit and healthy volunteers, were screened prior to participation, and those with any relevant medical history were excluded. The trial was registered on ISRCTN registry (ISRCTN16551998).<sup>17</sup>

After the screening appointment, all subjects received a 5 mm punch biopsy under local anaesthetic, to both upper inner arms, to create a uniform scar. The subjects were then divided into 4 groups, representing a temporal sequential time point, at 4, 8, 12, and 16 weeks. The subjects attended fortnightly appointment where non-invasive measurements (including OCT) were taken. At the first visit following the biopsy they were given both the treatment topical, and the positive control, with instructions on how to apply them. The subjects, and the trial clinician were blinded as to which arm received treatment or control. At their final appointment (dependent on group), the scar was excised via a 6 mm punch biopsy under local anaesthetic and at this point the subject exited the study.<sup>16</sup> All visits took places at University Hospital of South Manchester, part of Manchester University NHS Foundation Trust,

1  
2  
3 (Manchester, UK). Other outcomes of this study were published in another study by  
4  
5 our group.<sup>16</sup>  
6  
7  
8  
9

## 10 **Raman Spectroscopy**

11  
12 Biopsies were snap frozen and stored at -80 °C before use. They were sliced into  
13  
14 cross-sections of 10 µm thickness and mounted onto Raman-grade calcium fluoride  
15  
16 slides (Crystran Ltd, UK). Raman analysis was undertaken using a Renishaw inVia  
17  
18 confocal Raman microscope (Renishaw Plc., UK) equipped with a 785nm laser. The  
19  
20 instrument was calibrated using a silicon plate focused under a ×50 objective, where  
21  
22 a static spectrum centered at 520 cm<sup>-1</sup> for 1s at 10% power was collected.  
23  
24  
25  
26  
27  
28

29 Spectral data were collected using the WiRE 3.4 software (Galactic Industries Corp.,  
30  
31 USA). All spectra were acquired using the laser power adjusted on the sample to ~28  
32  
33 mW. An average of six static spectral point measurements were taken in each layer.  
34  
35 Data acquisition was optimised for our samples; using 100% power of the laser, with  
36  
37 ten second exposure time and ten accumulations (total measurement time of 100 s),  
38  
39 in order to analyse each point with the most optimal signal to noise. After data  
40  
41 collection any spurious spikes (cosmic rays) in the spectra, were removed using the  
42  
43 Cosmic Ray Removal function in WiRE. Raman spectra were truncated in the  
44  
45 fingerprint region (750-1800 cm<sup>-1</sup>), baseline corrected, scaled, and smoothed  
46  
47 (Savitzky-Golay filter) using MATLAB software version R2019b (The MathWorks Inc.,  
48  
49 USA). Area under the bands peaking at 1655 and 1446 cm<sup>-1</sup> were calculated using  
50  
51 in house scripts and the ratios 1655/1446 were tested by one-way ANOVA and  
52  
53 multiple compared using Tukey's test.  
54  
55  
56  
57  
58  
59  
60

## Histology

Formalin-fixed samples ( $n=16$  for each stain) were sectioned on a microtome into 5  $\mu\text{m}$  slices and placed onto glass slides. The slides were deparaffinised by xylene and rehydrated through grades of alcohol. Picrosirius Red staining was performed using Picro Sirius Red stain kit ab150681, (Abcam, USA). The Picrosirius Red staining was viewed by an Olympus BX63 microscope (Tokyo, Japan) for polarized images; collagen I was shown in red/orange and collagen III was shown in green/yellow. Elastin staining required antigen retrieval using 10% v/v citrate buffer, (Sigma Aldrich, Germany) for 20 min. Overnight incubation with 1:600 anti-elastin antibody, ab 23747, (Abcam, USA). Alexa Fluo 488 secondary antibody A-11034 (ThermoFisher, Germany) was added to the sections and incubated for 40 min. DAPI, 62248, (ThermoFisher, Germany) was used to counterstain. Sections were then dehydrated cleaned and mounted.

For Picrosirius Red, ImageJ was used to process the regions of interest, splitting the images into different color channels: red for collagen I quantification and green for collagen III. Analysis of elastin used Definiens Tissue Studio (Definiens, Germany) to quantify the region of interest. The frequency distribution of the collagen and elastin expression data was assessed by the Shapiro-Wilk normality test. All data passed the normality test and were evenly distributed. Subsequently, one-way ANOVA with repeated measurements was performed for both the collagen and elastin datasets. The mean collagen I/III ratio and the mean elastin level of each week were compared with the mean values of all other weeks. Differences were considered to be statistically significant when  $p < 0.05$ .

## Results

### HPLC and Mass Spectrometry

Following the methodology described above, the standard concentrations of both linoleic acid and tyramine were ascertained. Linoleic acid was present at ten times higher concentration, making it easier to detect; neither compound was present in the control topical (Figure 2A). To test the penetration of each compound, samples were sectioned longitudinally and correlated with H&E staining to ensure the correct dermal layer was identified for HPLC (Figure 2B). Whilst it is possible to detect linoleic acid in Day 0 (normal skin, no treatment) and in the samples which received the positive control, it was detected at much higher levels in treatment topical samples, although notably this peak was smaller with deeper penetration, where it can be presumed linoleic acid was present in much lower quantities. Tyramine was much more difficult to detect and was present in low quantities in all samples. In Figure 2C the average peak area of linoleic acid in the treatment samples is much greater, implying that it was easier to detect in *in vivo* samples. As with the *ex vivo* samples, the quantities detected were lower with deeper penetration, and the average peak area for tyramine was much lower, although still detectable in the day 0 and control samples. To validate the presence of both compounds, MS was used to detect linoleic acid and tyramine in treatment samples, the average concentration of both compounds is shown in Figure 2D.

### Raman spectroscopy

Measuring the spectra of the treatment topical, distinctive peaks were noted at 1042-1120, 1266-1303, 1439, and 1656  $\text{cm}^{-1}$  (Figure 3A) in the Raman spectra of samples treated with the topical, although all these peaks may account for lipid, protein, and

1  
2  
3 nucleic acids vibrations in 'normal' skin, (listed in 3B)<sup>18</sup> they were of higher attenuation.  
4  
5 Figures 3C and 3D demonstrate the spectra for *ex vivo* samples for day 0, the positive  
6  
7 control, and the treatment topical in the epidermis, and dermis, respectively. The  
8  
9 spectra are offset to facilitate visualisation, subtle changes are noted in the spectra of  
10  
11 dermis and epidermis collected from tissue submitted to treatment and positive control  
12  
13 compared to day 0.  
14  
15  
16  
17  
18

19 In Figure 4, the treatment topical skin spectra are represented at different time points,  
20  
21 in the epidermis and dermis. The time points represent the length of application of the  
22  
23 topical; i.e., for 4, 8, 12, or 16 weeks compared to baseline (day 0). As previously  
24  
25 described,<sup>19</sup> skin structures most relevant to scarring are visible at the amide I, amide  
26  
27 III, and proline bands. The amide I band represents collagen I in the dermis at 1665  
28  
29  $\text{cm}^{-1}$ , and at 1654  $\text{cm}^{-1}$  in the epidermis representing the  $\alpha$ -helix component of  
30  
31 keratin.<sup>20</sup> The amide III band is broad with a peak at 1246  $\text{cm}^{-1}$  associated with the  
32  
33 proline-rich (non-polar) and at 1271  $\text{cm}^{-1}$  proline-poor (polar) regions within  
34  
35 collagen.<sup>20</sup> Another band of note is at 1446  $\text{cm}^{-1}$  which is attributed to  $\text{CH}_2$  scissoring.<sup>21</sup>  
36  
37 Previous studies,<sup>21</sup> have demonstrated that the 1655/1446  $\text{cm}^{-1}$  band area ratio is  
38  
39 correlated to the collagen content. When applying this to the spectra collected at each  
40  
41 time point for the dermis in 4B, there is a significant decrease between the collagen  
42  
43 content at weeks 4, 12, and 16 ( $p < 0.05$ ), compared to day 0 (normal skin collagen  
44  
45 content); despite the rise in collagen content by week 16, it does not return to normal  
46  
47 levels.  
48  
49  
50  
51  
52  
53  
54  
55

56 Interestingly, at week 16 in the treated group, RS showed a shift of the amide I peak  
57  
58 from 1667  $\text{cm}^{-1}$  to 1656  $\text{cm}^{-1}$  in the dermis (Figure 5). This shift in the peak may  
59  
60

1  
2  
3 represent a change in protein conformation, from  $\beta$ -pleated sheets in elastin<sup>22</sup> in the  
4 region of  $1665\text{ cm}^{-1}$  to  $1675\text{ cm}^{-1}$  to a region of  $1650\text{ cm}^{-1}$  to  $1656\text{ cm}^{-1}$  which represents  
5  $\alpha$ -helix components of collagen.<sup>22</sup> Changes in the amide I peak representing  
6 secondary structural changes in protein have been recognised in skin previously:  
7 comparing normal skin to cancerous skin lesions<sup>23</sup> though not in the context of human  
8 skin scars. To corroborate these findings, traditional histology stains for collagen and  
9 elastin were carried out on skin scar samples which had the treatment topical applied  
10 for 4, 8, and 12 weeks. The images in the column on the left of Figure 6A represent  
11 Picro Sirius Red staining, imaged under polarised light. On day 0, there is an even  
12 distribution of collagen I and collagen III fibres. At weeks 4, and 8, there are more of  
13 the yellowish fibres of collagen III. At week 12, the distribution to collagen fibres is  
14 beginning to even out; 6B represents the ratio of collagen I/III fibres: at weeks 4 and  
15 8, this is significantly less than day 0, at week 12 this ratio was significantly higher than  
16 day 0 ( $p<0.0001$ ). The column on the right in 6A is anti-elastin antibody  
17 immunofluorescence staining. Even at week 12 there are very few elastin (green)  
18 fibres visible in the dermis. Figure 6C demonstrates a significant decrease ( $p<0.05$ )  
19 in elastin levels at week 4 compared to day 0, and despite a rise at week 8, there is a  
20 significant decrease ( $p<0.05$ ) also at week 12 compared to day 0. Whilst the RS  
21 collagen ratio does not demonstrate an increase to day 0 levels, the decrease in  
22 elastin and increase collagen over time fits with the process of fibrosis and  
23 corroborates with the shift in the amide I peak at week 16. Furthermore, clinical  
24 correlation using the OCT attenuation coefficient (Figure 6D) when volunteers had  
25 non-invasive measurements, there was a significant decrease in both treated and  
26 positive control arms compared to day 0 by week 4, which increased and was  
27  
28  
29  
30  
31  
32  
33  
34  
35  
36  
37  
38  
39  
40  
41  
42  
43  
44  
45  
46  
47  
48  
49  
50  
51  
52  
53  
54  
55  
56  
57  
58  
59  
60



1  
2  
3 significantly greater in the treated arm (compared to the control), at week 16 ( $p<0.05$ ),  
4  
5 (Figure 6E) though still not at baseline levels – as demonstrated using RS.  
6  
7  
8  
9  
10  
11  
12  
13  
14  
15  
16  
17  
18  
19  
20  
21  
22  
23  
24  
25  
26  
27  
28  
29  
30  
31  
32  
33  
34  
35  
36  
37  
38  
39  
40  
41  
42  
43  
44  
45  
46  
47  
48  
49  
50  
51  
52  
53  
54  
55  
56  
57  
58  
59  
60

## Discussion

Our study has demonstrated how HPLC and RS can be used to assess transdermal delivery of compounds, penetrating scar tissue even when the precise composition and mechanism of action of the topical remains unknown. Identifying penetration within each dermal layer is also possible using HPLC, but relies upon correlation of each section with H&E staining or careful tissue dissection. HPLC also relies on ensuring appropriate set up and usage of additional substances (solvents), although it has a higher signal sensitivity than RS (where techniques based on resonance or surface enhanced Raman scattering (SERS) must be employed to improve signal.<sup>24-</sup><sup>25</sup> HPLC also detected the overall concentration of the target compound in the whole sample, as it is based on the analysis of extracts; whilst Raman is complementary as it allows for the detection of levels of the compounds non-destructively in a spatial manner with a pixel resolution of  $\sim 1 \mu\text{m}$ . The use of cross-sectional samples whereby, under the high magnification of the confocal Raman microscope, dermal layers can be identified aids this process.

The novel finding of conformational changes within the scar tissue over sequential time points, could prove to be a major clinical benefit in the assessment of scarring, and provide additional objective and quantitative therapeutic assessment of topical formulations. RS requires minimal sample preparation or fixation and is non-destructive (unlike scanning electron microscopy (SEM), immunohistochemistry (IHC), or quantitative polymerase chain reaction (qPCR)), and requires no labelling, unlike some of these techniques. There is no loss of spatial information (as in mass spectrometry or qPCR), or sample processing (unlike western blots, qPCR, DNA microarrays) which is time consuming. RS is also cost-effective compared to more

1  
2  
3 traditional methods (however, we note that the instrument is costly, but after purchase  
4 no additional materials/chemicals are required). A combi-approach of HPLC with RS  
5 to evaluate clinical effects of the topical should therefore prove beneficial. Validation  
6 of this model using other techniques such as Fourier transform infrared (FTIR)  
7 microscopy, optical coherence tomography (OCT), high frequency ultrasound (HFUS),  
8 and traditional histology may also prove useful.  
9

10  
11  
12  
13  
14  
15  
16  
17  
18  
19 There is however, an ever-increasing role of RS in the clinical field, in terms of the  
20 skin, it has been used to assess functional effects of delivery of sunscreens<sup>26</sup> for  
21 example. RS has the capability of identifying the unique fingerprint of disease  
22 pathology, and changes within biomarkers in the skin.<sup>23</sup> Indeed, despite the huge  
23 clinical need for treatment for skin scarring, although there are a number of subjective  
24 scales for scar assessment<sup>3</sup> there is no current objective, and quantitative method for  
25 scarring classification and corresponding therapeutics.  
26  
27  
28  
29  
30  
31  
32  
33  
34  
35

36  
37  
38 There are limitations to this study: firstly, the reliance of the ability to section  
39 longitudinally through each dermal layer and accurately correlate with corresponding  
40 H&E sections in HPLC. It is also important to acknowledge that skin explants do not  
41 have the same permeability, elasticity, movement, and pharmacokinetics as intact  
42 skin, however our group have previously published work<sup>15</sup> (and more recently other  
43 groups)<sup>27-28</sup> demonstrating that it is possible to assess topical penetration on skin  
44 explants. The inability to use a true placebo compared to the treatment (since the  
45 treatment topical has no evidence to prove known actives) is another limitation,  
46 although in this case we were able to demonstrate how compounds could be identified  
47 in the absence known proven activity. Finally, we also acknowledge that the study  
48  
49  
50  
51  
52  
53  
54  
55  
56  
57  
58  
59  
60

1  
2  
3 has been conducted on a limited number of individuals and this to some degree is due  
4  
5 to the invasive sampling required to obtain tissue for HPLC and RS.  
6  
7  
8  
9

10 We have attempted to validate our RS results with histology and clinical correlation,  
11  
12 and although no direct comparisons can be made, we have demonstrated trends  
13  
14 within the different data sets. Extending the histology time points, and indeed the RS  
15  
16 analysis beyond weeks 12 and 16 respectively, to evaluate wound healing over a  
17  
18 longer time period, could provide more information. RS to our knowledge has not  
19  
20 been able to differentiate between Collagen I and Collagen III, although previous  
21  
22 studies have demonstrated a differentiation between types I and IV.<sup>19</sup> Collagen  
23  
24 differentiation has however been demonstrated using FTIR<sup>29</sup>. In both of these studies,  
25  
26 pure collagen was used (not from biological tissue).  
27  
28  
29  
30  
31  
32

33 Finally, although we have evidenced the treatment topical within the scarred skin  
34  
35 samples using RS, many of the compounds naturally exist within skin. The use of  
36  
37 SERS,<sup>30</sup> may help identify peaks not within the normal skin spectra which would aid  
38  
39 in removing this problem, but this is invasive as metallic nanoparticles need to be  
40  
41 added into the skin.  
42  
43  
44  
45  
46

47 We conclude that using RS, overcomes the difficulties in detecting topical-formulation  
48  
49 compounds at different depths using HPLC (i.e. the depth of penetration can be  
50  
51 quantified to ensure uniformity across all sections); and can be optimised to assess  
52  
53 the transdermal delivery of topicals through human skin scars. We have also  
54  
55 demonstrated the potential of RS for simultaneous evaluation of the effect of these  
56  
57  
58  
59  
60

1  
2  
3 compounds; with further evaluation of specific bands which may describe scar  
4  
5 composition.  
6  
7  
8  
9  
10  
11  
12  
13  
14  
15  
16  
17  
18  
19  
20  
21  
22  
23  
24  
25  
26  
27  
28  
29  
30  
31  
32  
33  
34  
35  
36  
37  
38  
39  
40  
41  
42  
43  
44  
45  
46  
47  
48  
49  
50  
51  
52  
53  
54  
55  
56  
57  
58  
59  
60

## Innovation

RS overcomes the difficulty in identifying compounds and positive penetration through scar tissue, validated by HPLC and MS; we have proved this is possible even when the composition of the topical is unknown. There is a role for RS in the clinical setting, where there is a lack of objective, and quantifiable means to assess scarring, and in monitoring therapeutic effects on scarring parameters by evaluation of structural changes within scar tissue. These findings can be corroborated by traditional techniques such as IHC, however RS is advantageous as it is non-destructive, does not require fixation or labelling, and easily replicable.

## Key findings

- A combi-approach of HPLC and RS can be used to assess transdermal delivery, even when the precise composition of a topical is unknown
- RS overcomes the difficulty of discriminating between dermal layers using HPLC, although HPLC has a higher signal sensitivity
- The novel detection of conformational changes using RS provides a role for its use in the clinical setting in the assessment of scarring and monitoring therapeutic effects of anti-scar topicals
- This combi-approach can be validated using more traditional techniques; MS to confirm the presence of compounds, IHC to confirm structural changes

### **Acknowledgments and funding sources**

Special thanks to Martin Isabelle, Renishaw Plc (UK) for Raman spectroscopy input and for test measurements carried out on RA816 Biological Analyser at Renishaw.

RB thanks Rehanna Sung, Manchester Institute of Biotechnology (UK), for HPLC analytical support. HM thanks the University of Liverpool for funding and support.

This project was partially funded by Julphar Gulf Pharmaceutical Industries, UAE and also by NIHR Manchester Biomedical Research Centre.



**Author disclosure and ghostwriting**

Rawya Al Kredy is an employee of Julphar Gulf Pharmaceutical Industries, UAE. No competing financial interests exist for all other authors with the exception of Rawya Al Kredy. The content of this article was expressly written by the authors listed. No ghostwriters were used to write this article.

**Abbreviations and acronyms**

FTIR	Fourier transform infrared
H&E	haematoxylin and eosin
HFUS	high frequency ultrasound
HPLC	high performance liquid chromatography
IHC	immunohistochemistry
MEBO	moist exposure burn ointment
MS	mass spectroscopy
OCT	optical coherence tomography
qPCR	quantitative polymerase chain reaction
RS	Raman spectroscopy
SEM	scanning electron microscopy
SERS	surface enhanced Raman scattering
WiRE	Windows-based Raman environment

## References

1. Sidgwick G, McGeorge D, Bayat A. A comprehensive evidence-based review on the role of topicals and dressings in the management of skin scarring. *Arch Dermatol Res* 2015; 207: 461-477.
2. Yildirimer L, Thanh NTK, Seifalian AM. Skin regeneration scaffolds: a multi-modal bottom-up approach. *Trends Biotechnol* 2012; 30: 638–648.
3. Markeson D, Pleat JM, Sharpe JR, Harris AL, Seifalian AM, Watt SM. Scarring, stem cells, scaffolds, and skin repair. *J Tissue Eng Regen Med* 2015; 9: 649-668
4. Bayat A, McGrouther DA. Spectrum of abnormal skin scars and their clinical management. *B J Hosp Med*. 2006; 67: 527-532
5. Mustoe TA, Gurjala A. The role of the epidermis and the mechanism of action of occlusive dressings in scarring. *Wound Repair Regen* 2011; 19: s16–s21
6. Dat AD, Poon F, Pham KB, Doust J. Aloe vera for treating acute and chronic wounds. *Cochrane Database Syst Rev* 2012 2:CD008762.
7. Curran JN, Crealey M, Sadadcharam G, Fitzpatrick G, O'Donnell M. Vitamin E: patterns of understanding, use, and prescription by health professionals and students at a university teaching hospital. *Plast Reconstr Surg* 2006; 118: 248–252
8. Ud-din S, Foden P, Mazhari M, et al. A double-blind randomized trial shows the role of zonal priming and direct topical application of epigallocatechin-3-gallate in the modulation of cutaneous scarring in human skin. *J Invest Dermatol* 2019; 139: 1680-1690
9. Majeed MUA. The Use of MEBO Scar Ointment in the treatment and prevention of post-operative wounds and scars. *Int J Pharm Res* 2016; 4: 1171-1178.

- 1  
2  
3 10. Zhang F, Erskine T, Klapacz J, Settivari R, Marty S. A highly sensitive and  
4  
5 selective high pressure liquid chromatography with tandem mass spectrometry  
6  
7 (HPLC/MS-MS) method for the direct peptide reactivity assay (DPRA). J  
8  
9 Pharmacol Toxicol Methods 2018; 94: 1-15  
10  
11
- 12 11. Pirot F, Kalia YN, Stinchcomb AL, Keating G, Bunge A, Guy RH.  
13  
14 Characterization of the permeability barrier of human skin *in vivo*. Proct Natl  
15  
16 Acad Sci USA 1997; 94: 1562-7  
17  
18
- 19 12. Essendoubi M, Gobinet C, Reynaud R, Angiboust JF, Manfait M, Piot O. Human  
20  
21 skin penetration of hyaluronic acid of different molecular weights as probed by  
22  
23 Raman Spectroscopy. Skin Res Tech 2016; 22: 56-52  
24  
25
- 26 13. Chan AKL, Zhang G, Tomic-Canic M, et al. A coordinated approach to  
27  
28 cutaneous wound healing: vibrational microscopy and molecular biology J Cell  
29  
30 Mol Med 2008; 2: 2145-2154  
31  
32
- 33 14. Binder L, SheikhRezaei S, Baierl A, Gruber L, Wolzt M, Valenta C. Confocal  
34  
35 Raman spectroscopy: in vivo measurement of physiological skin parameters –  
36  
37 A pilot study. J Dermatol Sci 2017; 88: 280-288  
38  
39
- 40 15. Sidgwick GP, McGeorge D, Bayat A. Functional testing of topical skin  
41  
42 formulations using an optimised ex vivo skin organ culture model. Arch  
43  
44 Dermatol Res 2016; 308: 297-306  
45  
46
- 47 16. Basson R, Baguneid M, Foden P, Al Kredly R, Bayat A. Functional testing of a  
48  
49 skin topical in vivo: objective and quantitative evaluation in human skin scarring  
50  
51 using a double-blind volunteer study with sequential biopsies. Adv Wound  
52  
53 Care 2019; 8: 208-219  
54  
55  
56  
57  
58  
59  
60

- 1  
2  
3 17. O'Brien L, Pandit A. Silicon gel sheeting for preventing and treating  
4 hypertrophic and keloid scars. *Cochrane Database Syst Rev* 2006;  
5 (1):CD003826  
6  
7  
8  
9
- 10 18. Movasaghi Z, Rehman S, Rehman IU. Raman spectroscopy of biological  
11 tissues. *App. Spectroscopy Rev* 2007; 42: 493-541  
12  
13
- 14 19. Nguyen TT, Gobinet C, Feru J, Brassart-Pasco S, Manfait M, Piot O.  
15 Characterization of type I and IV collagens by Raman microspectroscopy:  
16 Identification of spectral markers of the dermo-epidermal junction.  
17 *Spectroscopy: An Int J* 2012; 7: 421-427  
18  
19  
20  
21  
22
- 23 20. Frushour BG, Koenig JL. Raman scattering of collagen, gelatin, and elastin.  
24 *Biopolymers* 1975; 14: 379-391  
25  
26  
27
- 28 21. Liu H, Liu H, Deng X, et al. Raman spectroscopy combined with SHG gives a  
29 new perspective for rapid assessment of the collagen status in the healing of  
30 cutaneous wounds. *Anal. Methods*; 2016; 8: 3503–3510  
31  
32  
33  
34
- 35 22. Rygula A, Majzner K, Marzec KM, Kaczor A, Pilarczyk M, Baranska M. Raman  
36 spectroscopy of proteins: a review. *J Raman Spectrosc* 2013; 44: 1061-1076  
37  
38  
39
- 40 23. Feng X, Moy AJ, Nguyen HTM, et al. Raman biophysical markers in skin cancer  
41 diagnosis. *J Biomed Opt* 2018; 23: 1-10  
42  
43  
44
- 45 24. Chisanga M, Muhamadali H, Ellis DI, Goodacre R. Enhancing disease  
46 diagnosis: biomedical applications of surfaced-enhanced Raman scattering.  
47 *Applied Science* 2019; 9: 1163  
48  
49
- 50 25. Ellis DI, Cowcher DP, Ashton L, O'Hagan S, Goodacre, R. Illuminating disease  
51 and enlightening biomedicine: Raman spectroscopy as a diagnostic tool.  
52 *Analyst* 2013; 138: 3871-3884  
53  
54  
55  
56  
57  
58  
59  
60

- 1  
2  
3 26. Tippavajhala VK, Mendes TO, Martin, AA. *In vivo* human skin penetration study  
4 of sunscreens by confocal Raman Spectroscopy. *AAPS PharmSciTech* 2018;  
5 19: 753-759  
6  
7  
8  
9  
10 27. Liu H, Kang RS, Bagnowski K, et al. Targeting the IL-17 receptor using  
11 liposomal spherical nucleic acids as topical therapy for psoriasis. *J Invest*  
12 *Dermatol* 2019; *in press*: doi: 10.1016/j.jid.2019.06.146  
13  
14  
15  
16  
17 28. Anitua E, Troya M, Pino A. A novel protein-based autologous serum for skin  
18 regeneration. *J Cosmet Dermatol* 2019; *in press*: doi: 0.1111/jocd.13075  
19  
20  
21 29. Belbachir K, Noreen R, Gouspillou G, Petibois C. Collagen types analysis and  
22 differentiation by FTIR spectroscopy. *Anal Bioanal Chem* 2009; 395: 829-37  
23  
24  
25  
26 30. Kneipp K, Wang Y, Kneipp H, et al. Single molecule detection using surface-  
27 enhanced Raman scattering (SERS). *Phys Rev Lett* 1997; 78: 1667-1670.  
28  
29  
30  
31  
32  
33  
34  
35  
36  
37  
38  
39  
40  
41  
42  
43  
44  
45  
46  
47  
48  
49  
50  
51  
52  
53  
54  
55  
56  
57  
58  
59  
60

## Figure Legends

**Figure 1 Experimental workflow.** 1A describes the *ex vivo* work which was initially carried out. To validate the *ex vivo* findings, skin samples from a clinical trial using the same topicals (1B) were used to test the same techniques (HPLC, and RS). MS was then used to confirm the presence of both compounds which were detected in HPLC. Additional conformational changes demonstrated using RS were validated with histology stains for elastin and collagen, and clinically with OCT attenuation coefficient.

**Figure 2 Comparison of the detected concentrations of tyramine and linoleic acid in the topicals, and treated samples via HPLC and MS.** 2A demonstrates the presence of both compounds in the treatment topical, and neither in the positive control. 2B shows the results for HPLC on *ex vivo* samples (n=9): an average of the area under each peak (for linoleic acid and tyramine) was taken to quantify the detection of both compounds in each layer. 2C shows the results for HPLC on *in vivo* samples (n=15) using the average area under each peak for both compounds in each layer; as with 2B, tyramine is present in much lower quantities. In 2D the average concentration of each compound detected in the skin samples with the treatment topical applied (n=9) is shown. Key: D0 = day 0, normal skin, no treatment, Control = samples which received the positive control topical, Treatment = samples which received the treatment topical. E = epidermis, P = Papillary dermis, R = reticular dermis.

**Figure 3 RS of the treatment topical compared to the positive control and no topical.** 3A demonstrates the spectrum of the treatment topical with the key bands of

1  
2  
3 high attenuation highlighted. 3B is a table with the band assignments for the peaks  
4 present within the treatment topical which may also account for constituents of normal  
5 skin. 3C shows spectra for the treatment topical against day 0 and the positive control  
6 in the epidermis. 3D shows spectra for the treatment topical against day 0 and the  
7 positive control in the dermis. The spectra in 3C and 3D are offset to facilitate  
8 visualisation. There are changes within the bands at 1040-1120 and 1200-1320  $\text{cm}^{-1}$   
9 which are regions highlighted in the treatment topical in 3A.  
10  
11  
12  
13  
14  
15  
16  
17  
18  
19  
20

21 **Figure 4 RS of *in vivo* treated skin scar samples at different time points.**

22  
23  
24 4A: Day 0 (no treatment, normal skin), compared to skin scar samples with the  
25 treatment topical which had been applied for 4, 8, 12, and 16 weeks in the epidermis.  
26  
27

28 4B: Day 0 (no treatment, normal skin), compared to skin scar samples with the  
29 treatment topical which had been applied for 4, 8, 12, and 16 weeks in the dermis. In  
30 4A and 4B the spectra are offset to facilitate visualisation. Turkey's test was used to  
31 evaluate the significance of the band area ratio (1655/1446  $\text{cm}^{-1}$ ) relating to collagen  
32 content in 4C; distinct letters indicate statistically significant differences between the  
33 groups ( $p < 0.05$ ), i.e. weeks 4, 12, and 16 were statistically significant compared to day  
34 0.  
35  
36  
37  
38  
39  
40  
41  
42  
43  
44  
45  
46

47 **Figure 5 Protein conformational changes identified using RS at week 16 in**  
48 **treated samples.** A shift in the amide I peak representing  $\beta$ -sheet contribution of  
49 elastin to  $\alpha$ -helix component of collagen. RS therefore detected changes in wound  
50 healing and remodelling.  
51  
52  
53  
54  
55  
56  
57  
58  
59  
60



1  
2  
3 **Figure 6 Assessment of collagen and elastin using histology and clinical**  
4 **correlation with OCT.** 6A shows the polarised light images the Picrosirius stain for  
5 collagen on the left, and immunofluorescence stain for elastin on the right at day 0,  
6 weeks 4, 8, and 12. On the Picro Sirius stain, collagen I fibres stain red/orange, and  
7 collagen III yellow/green. Elastin fibres stain green with nuclei in blue. 6B  
8 demonstrates the collagen I/III ratio which is significantly decreased at weeks 4 and 8  
9 and increased at week 12 compared to day 0,\*\*\*  $p < 0.0001$ . 6C demonstrates the  
10 decrease in elastin at weeks 4 and 12 which was significant compared to day 0, \*  
11  $p < 0.05$ . 6D demonstrates use of the OCT device and the image from which the  
12 attenuation compensation is taken. The attenuation coefficient represents collagen  
13 deposition, which is significantly less in both arms compared to day 0 ( $p = 0.031$ ), then  
14 increases in both arms, with a significant increase in the treatment arm compared to  
15 the control at week 16 ( $p = 0.047$ ), although it has not quite returned to baseline (day  
16 0) levels (6E).  
17  
18  
19  
20  
21  
22  
23  
24  
25  
26  
27  
28  
29  
30  
31  
32  
33  
34  
35  
36  
37  
38  
39  
40  
41  
42  
43  
44  
45  
46  
47  
48  
49  
50  
51  
52  
53  
54  
55  
56  
57  
58  
59  
60

## About the authors

Rubinder Basson is a clinical doctor and surgical trainee in Manchester, currently undertaking a PhD in Plastics and Reconstructive Surgery Research at the University of Manchester, UK, under Dr Ardeshir Bayat.

Cassio Lima is a Post-doctoral Researcher in the Department of Biochemistry at the University of Liverpool, UK; he has a specialist interest in FTIR in skin.

Howbeer Muhamadali is a Research Associate in the Department of Biochemistry at the University of Liverpool, UK, with research in metabolomics investigations using a variety of analytical techniques.

Weiping Li is a Research Technician at the University of Manchester, UK, in the Bayat Research Lab.

Katherine Hollywood is an analytical chemist and Senior Experimental Officer for Synbiochem at the University of Manchester, UK.

Ludanni Li is a Masters student at the University of Manchester, UK, under Dr Ardeshir Bayat.

Mohamed Baguneid is the Chair of Surgery, Al Ain Hospital, SEHA, Abu Dhabi Emirate, UAE

Rawya Al Kredy works in R&D at Julphar Pharma, UAE.

Royston Goodacre is Professor in Biological Chemistry at the University of Liverpool, UK. He is a leading expert in metabolomics and RS and also editor-in-chief of the journal Metabolomics.

Ardeshir Bayat is a Clinician Scientist and Reader at the University of Manchester, UK, he is an active member of the Wound Healing Society and on the Board of Directors for the Wound Healing Foundation. He is Principal Investigator and corresponding author for this paper.

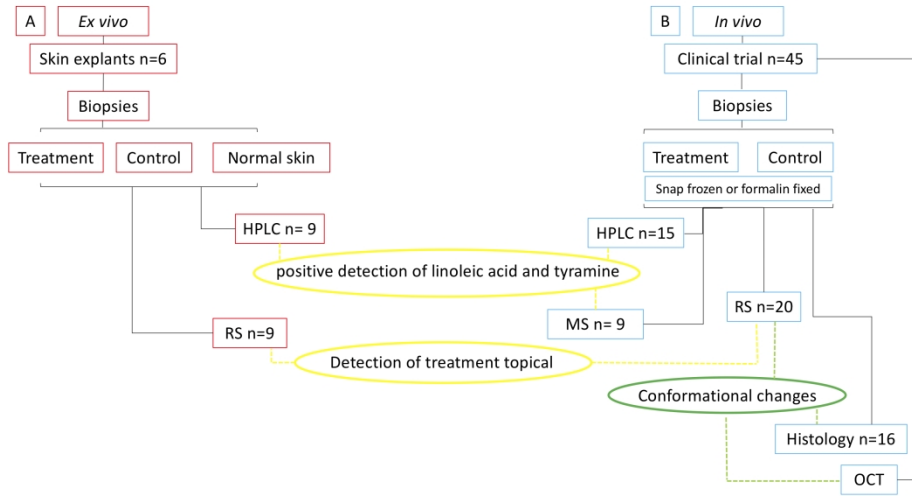


Figure 1 Experimental workflow. 1A describes the ex vivo work which was initially carried out. To validate the ex vivo findings, skin samples from a clinical trial using the same topicals (1B) were used to test the same techniques (HPLC, and RS). MS was then used to confirm the presence of both compounds which were detected in HPLC. Additional conformational changes demonstrated using RS were validated with histology stains for elastin and collagen, and clinically with OCT attenuation coefficient.

297x209mm (300 x 300 DPI)

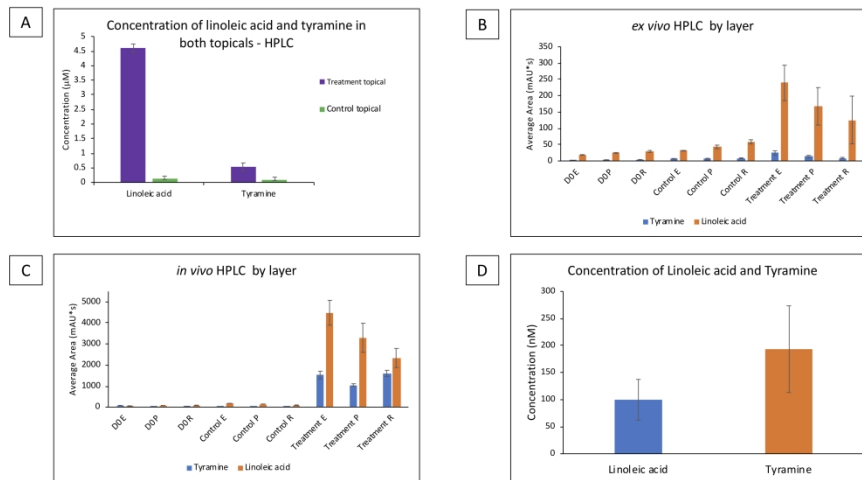


Figure 2 Comparison of the detected concentrations of tyramine and linoleic acid in the topicals, and treated samples via HPLC and MS. 2A demonstrates the presence of both compounds in the treatment topical, and neither in the positive control. 2B shows the results for HPLC on ex vivo samples (n=9): an average of the area under each peak (for linoleic acid and tyramine) was taken to quantify the detection of both compounds in each layer. 2C shows the results for HPLC on in vivo samples (n=15) using the average area under each peak for both compounds in each layer; as with 2B, tyramine is present in much lower quantities. In 2D the average concentration of each compound detected in the skin samples with the treatment topical applied (n=9) is shown. Key: D0 = day 0, normal skin, no treatment, Control = samples which received the positive control topical, Treatment = samples which received the treatment topical. E = epidermis, P = Papillary dermis, R = reticular dermis.

297x209mm (300 x 300 DPI)

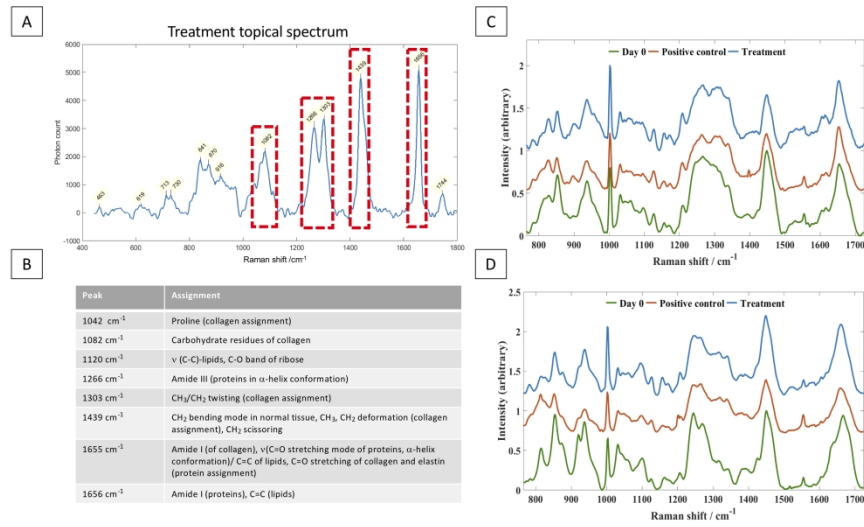


Figure 3 RS of the treatment topical compared to the positive control and no topical. 3A demonstrates the spectrum of the treatment topical with the key bands of high attenuation highlighted. 3B is a table with the band assignments for the peaks present within the treatment topical which may also account for constituents of normal skin. 3C shows spectra for the treatment topical against day 0 and the positive control in the epidermis. 3D shows spectra for the treatment topical against day 0 and the positive control in the dermis. The spectra in 3C and 3D are offset to facilitate visualisation. There are changes within the bands at 1040-1120 and 1200-1320  $\text{cm}^{-1}$  which are regions highlighted in the treatment topical in 3A.

297x209mm (300 x 300 DPI)

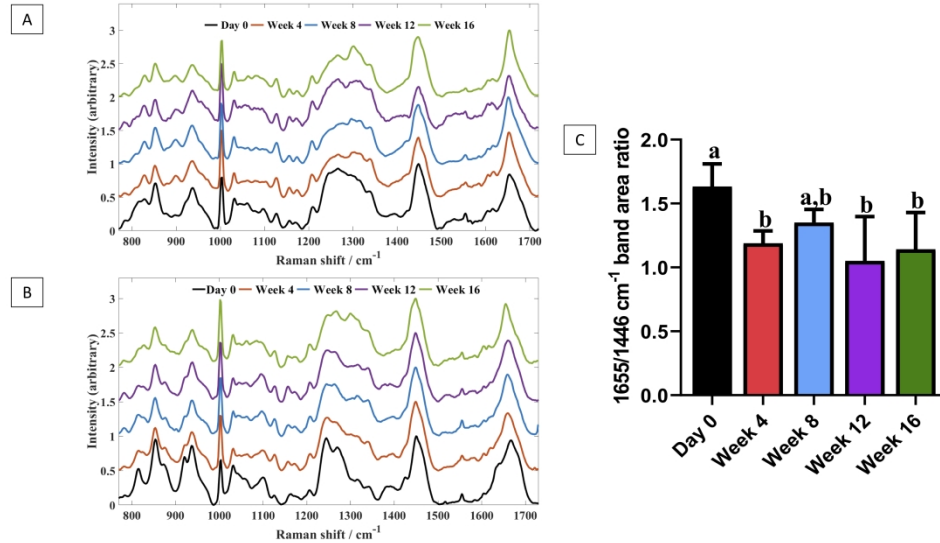


Figure 4 RS of in vivo treated skin scar samples at different time points.

4A: Day 0 (no treatment, normal skin), compared to skin scar samples with the treatment topical which had been applied for 4, 8, 12, and 16 weeks in the epidermis. 4B: Day 0 (no treatment, normal skin), compared to skin scar samples with the treatment topical which had been applied for 4, 8, 12, and 16 weeks in the dermis. In 4A and 4B the spectra are offset to facilitate visualisation. Turkey's test was used to evaluate the significance of the band area ratio (1655/1446 cm<sup>-1</sup>) relating to collagen content in 4C; distinct letters indicate statistically significant differences between the groups ( $p < 0.05$ ), i.e. weeks 4, 12, and 16 were statistically significant compared to day 0.

297x209mm (300 x 300 DPI)

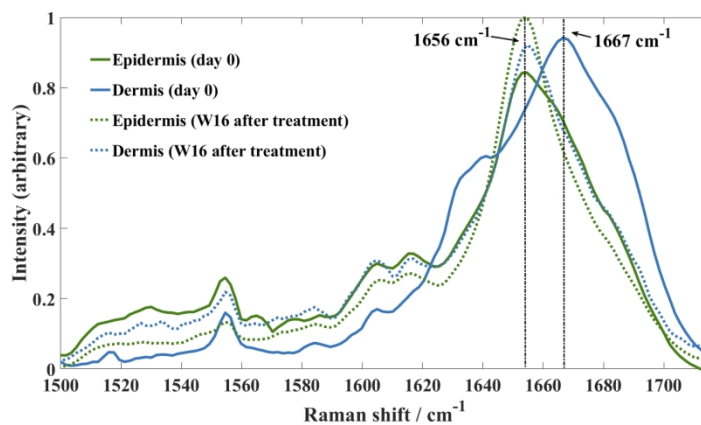


Figure 5 Protein conformational changes identified using RS at week 16 in treated samples. A shift in the amide I peak representing  $\beta$ -sheet contribution of elastin to  $\alpha$ -helix component of collagen. RS therefore detected changes in wound healing and remodelling.

297x209mm (300 x 300 DPI)

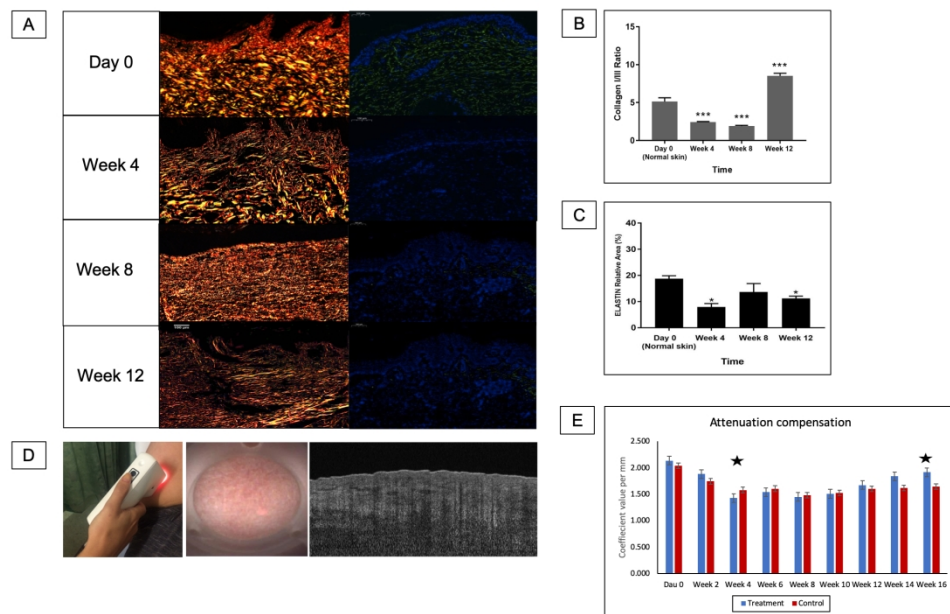


Figure 6 Assessment of collagen and elastin using histology and clinical correlation with OCT. 6A shows the polarised light images the Picosirius stain for collagen on the left, and immunofluorescence stain for elastin on the right at day 0, weeks 4, 8, and 12. On the Picro Sirius stain, collagen I fibres stain red/orange, and collagen III yellow/green. Elastin fibres stain green with nuclei in blue. 6B demonstrates the collagen I/III ratio which is significantly decreased at weeks 4 and 8 and increased at week 12 compared to day 0, \*\*\*  $p < 0.0001$ . 6C demonstrates the decrease in elastin at weeks 4 and 12 which was significant compared to day 0, \*  $p < 0.05$ . 6D demonstrates use of the OCT device and the image from which the attenuation compensation is taken. The attenuation coefficient represents collagen deposition, which is significantly less in both arms compared to day 0 ( $p=0.031$ ), then increases in both arms, with a significant increase in the treatment arm compared to the control at week 16 ( $p=0.047$ ), although it has not quite returned to baseline (day 0) levels (6E).

187x121mm (300 x 300 DPI)





Corresponding author photo: Dr Ardeshir Bayat

151x138mm (150 x 150 DPI)